

UC Berkeley

UC Berkeley Previously Published Works

Title

Electrical switching of the magnetic vortex circulation in artificial multiferroic structure of Co/Cu/PMN-PT(011)

Permalink

<https://escholarship.org/uc/item/9m57t2t0>

Journal

Applied Physics Letters, 110(26)

ISSN

0003-6951

Authors

Li, Q
Tan, A
Scholl, A
[et al.](#)

Publication Date

2017-06-26

DOI

10.1063/1.4990987

Peer reviewed

Electrical switching of the magnetic vortex circulation in artificial multiferroic structure of Co/Cu/PMN-PT(011)

Q. Li, A. Tan, A. Scholl, A. T. Young, M. Yang, C. Hwang, A. T. N'Diaye, E. Arenholz, J. Li, and Z. Q. Qiu

Citation: *Appl. Phys. Lett.* **110**, 262405 (2017); doi: 10.1063/1.4990987

View online: <https://doi.org/10.1063/1.4990987>

View Table of Contents: <http://aip.scitation.org/toc/apl/110/26>

Published by the [American Institute of Physics](#)

Articles you may be interested in

[As-grown two-dimensional MoS₂ based photodetectors with naturally formed contacts](#)

Applied Physics Letters **110**, 261109 (2017); 10.1063/1.4990968

[Manipulation of anisotropic magnetoresistance and domain configuration in Co/PMN-PT \(011\) multiferroic heterostructures by electric field](#)

Applied Physics Letters **111**, 052401 (2017); 10.1063/1.4997322

[Electrode modulated capacitance-electric field nonlinearity in metal-insulator-metal capacitors](#)

Applied Physics Letters **110**, 263503 (2017); 10.1063/1.4989531

[Extraordinary optical transmission through nonlocal holey metal films](#)

Applied Physics Letters **110**, 261110 (2017); 10.1063/1.4991016

[Magnetoelectric write and read operations in a stress-mediated multiferroic memory cell](#)

Applied Physics Letters **110**, 222401 (2017); 10.1063/1.4983717

[Electric-field tuning of ferromagnetic resonance in CoFeB/MgO magnetic tunnel junction on a piezoelectric PMN-PT substrate](#)

Applied Physics Letters **111**, 062401 (2017); 10.1063/1.4997915

PHYSICS TODAY

WHITEPAPERS

MANAGER'S GUIDE

Accelerate R&D with
Multiphysics Simulation

READ NOW

PRESENTED BY

 COMSOL

Electrical switching of the magnetic vortex circulation in artificial multiferroic structure of Co/Cu/PMN-PT(011)

Q. Li,¹ A. Tan,¹ A. Scholl,² A. T. Young,² M. Yang,¹ C. Hwang,³ A. T. N'Diaye,² E. Arenholz,² J. Li,^{4,a)} and Z. Q. Qiu^{1,a)}

¹Department of Physics, University of California at Berkeley, Berkeley, California 94720, USA

²Advanced Light Source, Lawrence Berkeley National Laboratory, Berkeley, California 94720, USA

³Korea Research Institute of Standards and Science, Yuseong, Daejeon 305-340, Korea

⁴International Center for Quantum Materials and School of Physics, Peking University, Beijing 100871, China

(Received 5 April 2017; accepted 18 June 2017; published online 30 June 2017)

Co films and micron sized disks were grown on top of piezoelectric PMN-PT(011) and Cu/PMN-PT(001) substrates and investigated by the Magneto-Optic Kerr Effect and Photoemission Electron Microscopy. By applying an electric field in the surface normal direction, we find that the strain of the ferroelectric PMN-PT(011) substrate induces an in-plane uniaxial magnetic anisotropy in the Co overlayer. Under specific conditions, the Co magnetic vortex could be switched between clockwise and counter-clockwise circulations. The variations of the Co vortex switching were attributed to the variations of the ferroelectric domains under the Co disks. We speculate that the switching of the magnetic vortex circulation is a dynamical process which may involve pulses of appropriate magnitude and duration of the uniaxial magnetic anisotropy delivered to the magnetic vortex. Published by AIP Publishing. [<http://dx.doi.org/10.1063/1.4990987>]

The non-volatility of magnetic memory makes it an ideal candidate for information storage.¹ Moreover, devices based on magnetic architectures are intrinsically more energy-efficient than conventional transistors because of the absence of leakage current. Therefore, it has been important and desirable to achieve a switching of the magnetization by an external voltage/electric field for both fundamental research and technological applications.² Among variable approaches, multiferroic-magneto-electric composite systems, either naturally formed components or artificial ferromagnetic (FM)/ferroelectric (FE) heterostructures, have been explored extensively due to the coupling between the ferroelectric and magnetic orders.^{3,4} In particular, the magnetoelectric effect in FM/FE heterostructures is very promising because piezostain produced by an electric field in the FE layer could be easily transferred to the FM layer in a heterostructure. Devices based on this principle are estimated to have 3–5 orders of magnitude more energy efficiency than the conventional transistors.^{5,6} It was also proposed that magnetization could be switched by low voltages in a single-domain nanomagnet with little energy dissipation.⁷

Phenomenologically, the influence of strain on the magnetostrictive layer is a spin reorientation transition (SRT) of the thin-film magnetization from in-plane to out-of-plane directions.^{8,9} More recently, however, ferroelastic (71°, 109°) domain switching was observed in new generation single-crystal ferroelectrics $\text{Pb}(\text{Zn}_{1/3}\text{Nb}_{2/3})\text{O}_3\text{-PbTiO}_3$ (PZN-PT) and $\text{Pb}(\text{Mg}_{1/3}\text{Nb}_{2/3})\text{O}_3\text{-PbTiO}_3$ (PMN-PT). The unique switching pathways in these materials induce an in-plane strain anisotropy, thus leading to an in-plane 90° magnetization switching by applying an out-of-plane electric field.^{10–14}

It was also proposed¹⁵ and shown experimentally^{16,17} that a single domain nanomagnet could be switched by electric voltage between two states of orthogonal in-plane orientations. Furthermore, it was demonstrated that the domain walls of a magnetic vortex could be displaced by piezoelectric strain in Ni nanostructured squares grown on PNM-PT.¹⁸ However, it is unclear how the strain from the substrate is transferred to the ferromagnetic layer across a 50 nm thick Pt spacer layer. Despite the above progress, it has not yet realized a clean and reliable voltage switching of magnetization between two opposite directions which are desired binary memory states. An alternative approach is to seek voltage switching between two different magnetic domain states, e.g., switching of magnetic vortex states between opposite circulations. The vortex circulation is characterized by the in-plane curling of the magnetization vector (clockwise or counter-clockwise) around the center of the vortex and has been proposed as the possible binary memory states. The control of vortex circulation has been realized via means other than the electric voltage such as by an asymmetry in the structure shape,¹⁹ the spatial distribution of the applied magnetic field,^{20,21} nanosecond magnetic field pulse,²² and by exchange bias.²³ Regarding the electric control of vortex domain states, it was reported very recently that elliptical Co nanomagnets could be driven from a single domain state into a vortex state by surface acoustic waves, which modulates the stress anisotropy of these nanomagnets.²⁴ But unfortunately, such switching is not the desired binary vortex states of opposite circulations. Until now, voltage controlled circulation switching of a vortex state has been rarely reported either theoretically or experimentally. In this article, we report evidence of electric switching of the magnetic vortex state in the Co/Cu/PMN-PT(011) system. First, we studied uniaxial magnetic anisotropy of Co films induced by piezostain of the PMN-PT

^{a)}jiali83@pku.edu.cn and qiu@berkeley.edu

substrate. Then, we demonstrate that the circulation of a Co magnetic vortex could be switched by applying an out-of-plane electric field to the PMN-PT substrate.

A 0.5-mm-thick PMN-PT(011) single crystalline substrate was annealed in an ultrahigh vacuum with a base pressure of 2×10^{-10} Torr to a temperature of 600°C . Then, Copper (Cu) films of various thicknesses (0, 2, 4, and 15 nm) were grown on top of the PMN-PT(011) at room temperature by moving the sample holder behind a knife-edge shutter, followed by a 30 nm thick Co film grown from an e-beam evaporator. Finally, a 2 nm Cu film was capped as a protection layer. This metallic upper layer also served as a top electrode. Another 15 nm thick Cu layer was grown on the back-side of the PMN-PT(011) substrate to serve as the back electrode so that the electric field can be applied to the PMN-PT in the out-of-plane direction by applying a voltage between the top and the back electrodes.

Figure 1(a) shows the experimental geometry for the Magneto-optical Kerr effect (MOKE) measurement. In addition to the conventional hysteresis loop measurement, we also performed the rotation MOKE (ROTMOKE) measurement to determine the magnetic anisotropy of the Co films. For the ROTMOKE measurement, a 300-Oe magnetic field rotates in the film plane to rotate the Co magnetization. As an example, Fig. 2(b) shows the normalized Kerr signal as a function of in-plane magnetic field angle θ_H , which almost follows the cosine curve for an electric field of 0.35 MV/m and deviates from the cosine curve for an electric field of 1.0 MV/m. Since MOKE measures the projection of the in-plane magnetization in the optical plane [x-axis or $[0\bar{1}1]$ -axis of the PMN-PT crystal shown in Fig. 1(b)], the angular difference between the magnetization and the magnetic field permits the determination of the magnetic anisotropy of the Co film. For our case, we only need to consider the Zeeman energy and the voltage induced uniaxial magnetic anisotropy because the polycrystalline Co film averages out any preferred direction of the Co magnetization due to its own magnetic anisotropy. Then, the gross energy density of the system is given by

$$E_V = -M_S H \cos(\theta_H - \theta_M) + K_2 \sin^2(\theta_M). \quad (1)$$

Here, E_V is the energy density, $M_S = 1400 \text{ emu/cm}^3$ is the Co saturation magnetization, H is the external magnetic field, θ_H and θ_M are the angles of the magnetic field and Co magnetization relative to the x-axis, and K_2 is the strain-induced uniaxial anisotropy constant. The direction of

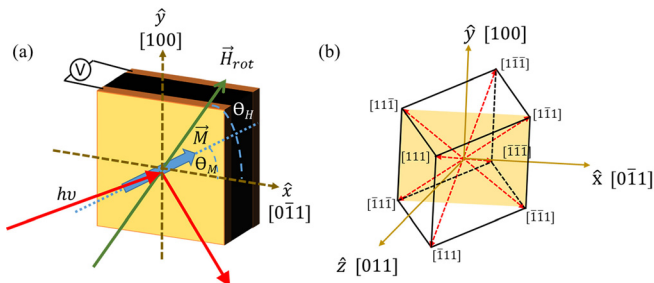


FIG. 1. (a) Experimental geometry for uniaxial anisotropy measurements for Co/PMN-PT(011) under a perpendicularly applied electric field using ROTMOKE. (b) Sketch of the PMN-PT(011) crystal structure.

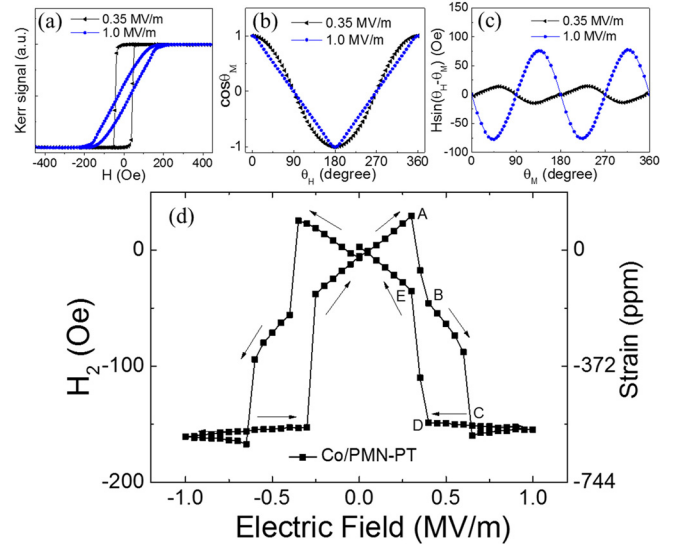


FIG. 2. (a) Hysteresis loops measured at 0.35 MV/m and 1.0 MV/m applied electric field along the $[0\bar{1}1]$ axis. (b) Kerr signal as a function of magnetic field angle θ_H . (c) Magnetic torque $H \sin(\theta_H - \theta_M)$ experienced by the magnetization as a function of magnetization angle θ_M . (d) Uniaxial magnetic anisotropy field (left axis) and transferred strain (right axis) as a function of applied electric field strength.

magnetization can be obtained by minimizing the energy density with respect to the magnetization angle $\frac{\partial E_V}{\partial \theta_M} = 0$

$$-M_S H \sin(\theta_H - \theta_M) + K_2 \sin 2\theta_M = 0. \quad (2)$$

Defining the magnetic torque of $L(\theta_M) = H \sin(\theta_H - \theta_M)$ and substituting with $2K_2/M_S = H_2$, we obtain

$$L(\theta_M) = K_2 \sin 2\theta_M / M_S \equiv \frac{1}{2} H_2 \sin 2\theta_M. \quad (3)$$

By fitting the experimental value of the magnetic torque using Eq. (3), the uniaxial anisotropy field of H_2 can be retrieved.^{12,25}

Figure 2 shows the result of the strain induced uniaxial anisotropy in a 30-nm Co film grown on the PMN-PT(011) substrate at different applied electric field values. First, Fig. 2(a) clearly shows that the hysteresis loops change from square-shape to hard-axis loops after changing the electric field from 0.35 MV/m to 1.0 MV/m. This easy-axis (EA) magnetization switching is further reflected by the 90° shift of the magnetic torque curve in Fig. 2(c). The fitted uniaxial anisotropy field $H_2 = 155 \text{ Oe}$ with the EA along the $[100]$ axis at an applied electric field of 1.0 MV/m and a fitted uniaxial anisotropy $H_2 = 29 \text{ Oe}$ with EA along the $[0\bar{1}1]$ axis at an applied electric field of 0.35 MV/m are revealed by the blue and black torque curves in Fig. 2(c), respectively, similar to the results reported in the literature.^{8,12,26} The magnetic anisotropy field H_2 exhibits a symmetric butterfly shape as a function of the electric field [Fig. 2(d)] which has been attributed to the stain-induced magnetic anisotropy.^{12–14,27} The absence of the magnetic anisotropy at the zero electric field is an indication of the zero strain in the polycrystalline Co film. With increasing the electric field, the ferromagnetic thin film first shows a positive uniaxial anisotropy with the EA parallel to the $[0\bar{1}1]$ axis and then switches to a negative value at around the 0.35 MV/m with

the EA parallel to the [100] axis. As the electric field further increases, the magnitude of the uniaxial anisotropy has another jump at around 0.6 MV/m and finally saturates above 0.65 MV/m of the applied electric field. The uniaxial anisotropy displays a hysteresis and a symmetric behavior for positive and negative electric field values. To confirm this butterfly shape behavior, we repeated the measurement by rotating the sample by 90° in-plane. The measured uniaxial anisotropy has the same value except for a sign change, confirming that the result is not due to any optical effect of the ROTMOKE. The butterfly shape of the uniaxial magnetic anisotropy is a strong reminiscence of the piezostrain of the substrate in response to the applied electric field. To discuss this mechanism more quantitatively, we employ the following relation between the magnetic anisotropy and the strain:^{8,16,18}

$$K_2 = -\frac{3}{2}\lambda_S Y |\epsilon_x - \epsilon_y|. \quad (4)$$

Here, $\lambda_S = 60$ ppm is the magnetostrictive constant of Co, $Y = 209$ GPa is the Young's modulus of Co, and $|\epsilon_x - \epsilon_y|$ is the in-plane strain difference between the piezoelectric response in the x- and y- directions due to the transverse electric field applied in the z direction. For the Co film at the saturation electric field, the induced magnetic uniaxial anisotropy energy is $K_2 = 2.17 \times 10^5$ erg/cm³ according to the relation to H_2 as $K_2 = \frac{1}{2}H_2M_S$. Then, using Eq. (4), we estimate an in-plane strain difference of $|\epsilon_x - \epsilon_y| \sim 623$ ppm in the Co film at the saturating electric field. This value is smaller than that of PMN-PT, indicating that some strain from the substrate is already relaxed in the Co film.

The behavior of the Co uniaxial anisotropy can be understood as follows. The Co film was grown on top of the PMN-PT(011) substrate in its remanent state which consists of ferroelectric domains that are randomly distributed along the 8 equivalent $\langle 111 \rangle$ easy axis orientations.^{12,13} At this state, the as-grown polycrystalline Co film contains no (or very small) in-plane magnetic anisotropy. As an electric field is applied along the z direction, the polarization of the ferroelectric substrate prefers to switch to the two out-of-plane $\langle 111 \rangle$ directions [$[\bar{1}\bar{1}\bar{1}]$ and $[1\bar{1}\bar{1}]$ directions in Fig. 1(b)] due to the rhombohedral phase, leading to an outstretched strain along the [100] axis and a compressive stain along the $[0\bar{1}\bar{1}]$ axis.^{13,16,18} Considering the positive sign of the Co magnetostrictive constant, the Co film obtains a uniaxial magnetic anisotropy with EA pointing along the direction of tensile strain, i.e., [100] axis. This strain induced EA orientation corresponds to the hard axis in the Ni/PMN-PT(110) system because Ni has a negative magnetostrictive constant.^{16,18} The two-step jumps of $A \rightarrow B \rightarrow C$ in Fig. 2(c) are then associated with the existence of the monoclinic phase, which bridges the reversal of domains of the rhombohedral phase during the bipolar cyclic electric field process.^{28,29}

The piezostrain mechanism of the induced magnetic anisotropy is further supported by inserting a copper spacer layer between the ferromagnetic Co layer and the ferroelectric PMN-PT(011) substrate. Figure 3 shows that the Cu spacer layer reduces the magnitude of the induced magnetic anisotropy, whereas the curve shape of the uniaxial

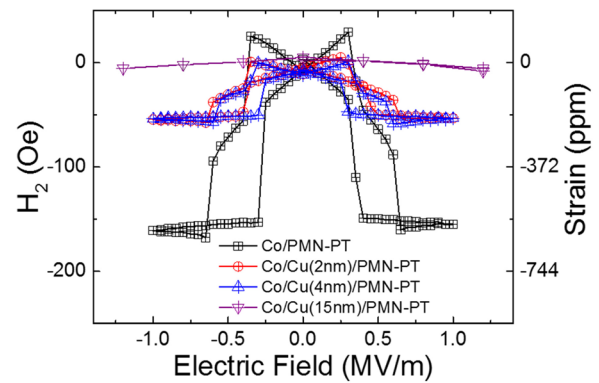


FIG. 3. Uniaxial anisotropy as a function of the applied electric field of Co(30 nm)/Cu(0, 2, 4, and 15 nm)/PMN-PT(011) with different thicknesses of the Cu spacer layer.

anisotropy versus electric field appears to be identical between 0, 2, and 4 nm of copper spacer thicknesses. The induced magnetic anisotropy is the largest when the ferromagnetic Co film is in direct contact with the ferroelectric PMN-PT(011) and decreases by about 67% for 2-nm and 4-nm Cu spacer layers and almost vanishes for the 15-nm Cu spacer layer. Recognizing that the strain relaxes with increasing Cu thickness, the result of Fig. 3 supports the piezostrain mechanism of the uniaxial magnetic anisotropy in the Co film.

To study the effect of induced uniaxial anisotropy on the vortex state, we prepared the Co (30 nm)/Cu spacer (0, 4 nm)/PMN-PT(011) sample. The Co layer here is patterned into ~ 1.5 μm diameter disks by evaporating Co through a contact shadow mask [Fig. 4(a)]. Element-resolved X-ray Magnetic Circular Dichroism (XMCD) was measured at the Advanced Light Source of Lawrence Berkeley National Laboratory at the Co 2p level at BL11.0.1.1. Circular polarized x-rays experience different absorption intensities at the $L_{3,2}$ edges for magnetization parallel and antiparallel to the X-ray beam. Thus, from the element-resolved Photoemission Electron Microscopy (PEEM) images, one can retrieve the Co domain patterns as well as their relative magnetization directions.

Figures 4(c) and 4(d) show the domain images as a function of different applied electric fields for Co disks on the PMN-PT(011) substrate from two different disks. A transition was observed at 0.2 MV/m electric field with the magnetization changes to the direction perpendicular to the x-ray beam (the up/down in-plane direction in Figs. 4(c) and 4(d) so that the magnetic contrast diminishes). Further increasing the electric field to 0.4–0.6 MV/m leads to a vortex with the magnetization direction more or less parallel to the x-ray beam [light/right in plane directions in Figs. 4(c) and 4(d)]. Above 0.8 MV/m electric field, some of the magnetic vortices become single domain state, while others remain vortices with half-left and half-right magnetization directions. The above observations are consistent with the ROTMOKE result that the uniaxial anisotropy first becomes positive and then negative before fully saturating. It should be mentioned that to ensure a good conductive upper electrode for the electric field application and a good conducting surface for the PEEM operation, a 10-nm Cu capping layer was deposited on the whole sample after the magnetic Co disks were

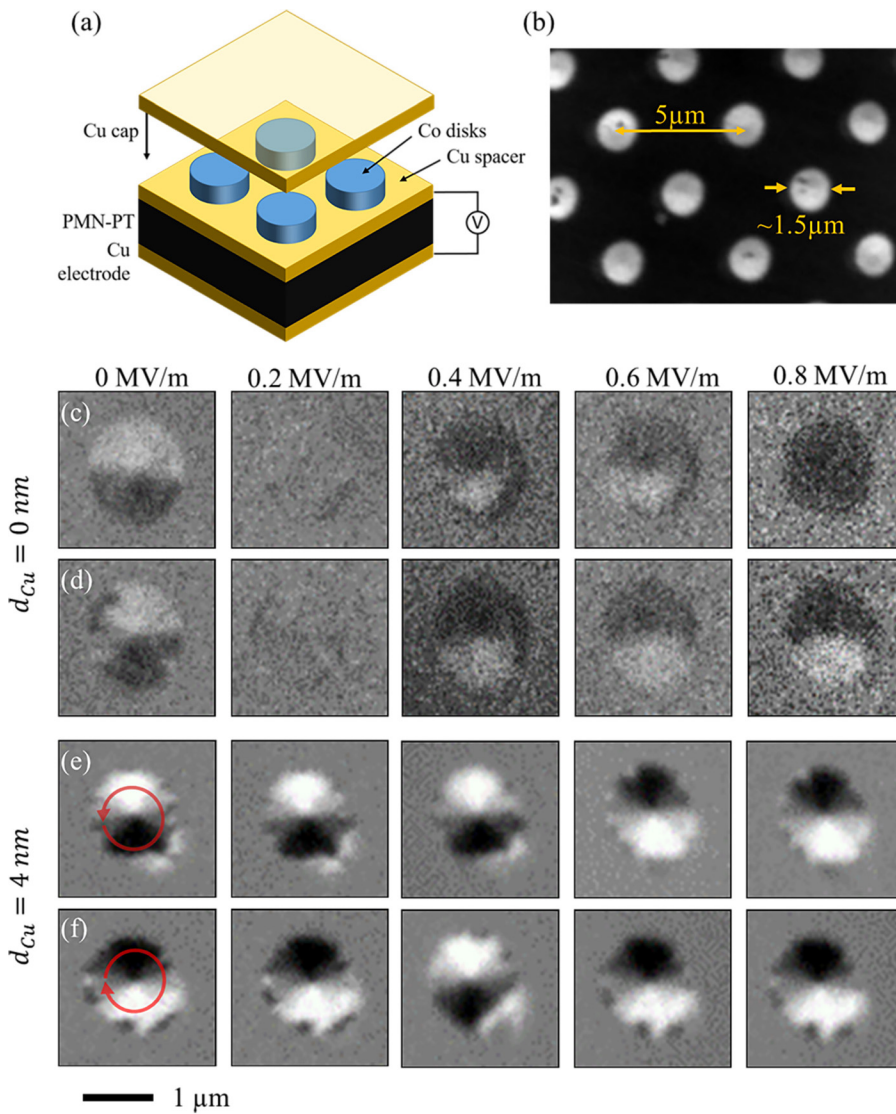


FIG. 4. (a) A sketch of the sample structure for PEEM measurements. (b) A PEEM image of the Co L_3 edge showing the formation of Co disks. A series of XMCD images taken using PEEM, where the applied voltages were increased from 0 MV/m to 0.8 MV/m in step of 0.05 MV/m of (c) and (d) Co/PMN-PT(011) and (e) and (f) Co/Cu(4 nm)/PMN-PT(011). The applied voltage listed for each image was held constant while PEEM images were taken. Vortex circulation switchings are clearly seen.

grown. This relatively thick Cu layer results in a less magnetic contrast from the Co disk due to the finite escaping depth of the electrons in the PEEM measurement. Nevertheless, we were still able to obtain the weak Co magnetic contrast although it is difficult to perform a quantitative analysis on the Co domain contrast and the domain area. The interesting observation is that some vortices switch their circulation in the 0.4–0.6 MV/m electric field range as compared to their original circulations. To further explore this phenomenon, we imaged Co (30 nm disks)/Cu (4 nm)/PMN-PT(011) at different electric fields from two different Co disks [Figs. 4(e) and 4(f)]. The better XMCD contrasts in Figs. 4(e) and 4(f) are due to the fact that the presence of the Cu spacer layer in this sample allows a thinner copper capping layer as the top electrode, thus permitting more secondary electrons to escape. The Co disks with a 4-nm Cu spacer layer exhibit clearly a vortex state of equally distributed four domains areas instead of two domains from Co disks in direct contact with the PMN-PT substrate in Figs. 4(c) and 4(d), confirming the attenuation of stain-induced anisotropy in Co disks with a thicker Cu spacer layer, which is consistent with the ROTMOKE result of the Co film shown in Fig. 3. The most interesting result is that the circulation of the Co magnetic vortex switches from counter-clockwise to

clockwise as the applied electric field is increased from 0.4 MV/m to 0.6 MV/m [Fig. 4(e)]. On another disk [Fig. 4(f)], we observed the circulation switching from clockwise to counter-clockwise from 0.2 MV/m to 0.4 MV/m, but resume to clockwise circulation when the electric field is further increased to 0.6 MV/m. There exist both “randomness” and “reproducibility” in the circulation switching. The “randomness” is reflected by the following two facts: (1) among all disks, it is random on which disks switch and which do not and (2) the circulation switching is different from disk to disk, sometimes the switching occurs during the increasing stage of the voltage and sometimes the switching occurs during the decreasing stage of the voltage. The “reproducibility” is reflected by the following two facts: (1) the switched vortex is stable, i.e., retains its circulation rather than switching back and forth with time and (2) the switching always occurs at the 0.2–0.5 MV/m electrical field which corresponds to the ferroelectrical coercivity of the PMN-PT. It is actually somewhat expected that there is no specific correspondence between the electric field and the sign of the vortex circulation because an out-of-plane electrical field should not break the clockwise and counterclockwise circulations. Nevertheless, we demonstrate clearly that an electric field could switch the circulation of a magnetic vortex.

The different behavior of these ferromagnetic disks could be due to either the inhomogeneity of these disks or more likely the presence of small sized ferroelectric domains in PMN-PT(110). The ferroelectric domain size in PMN-PT (011) could range from submicron to micron, which is comparable and smaller than the size of our Co disk.^{16,18} Since the ROTMOKE measurement is performed with a He-Ne laser, the measured uniaxial anisotropy represents the averaged property over a rather large area covered by the laser beam size (approximately 300 μm of diameter). Therefore, uniaxial anisotropy determined by ROTMOKE represents the collective behavior of many ferroelectric domains, whereas the strain transferred to a single ferromagnetic disk would depend on the details of the ferroelectric domain configurations below the disk. This explains why there exist different switching processes of the same sized Co disks. Unfortunately, we could not image the ferroelectric domains in experiment so have to leave it to future studies on the microscopic relation between the Co vortex state and the underlying ferroelectric domain when there are available experiment techniques. From the general argument, the nature of time-reversal symmetry of electric field should not lead to a uniquely determined 180-degree magnetization switching which breaks the time-reversal symmetry. This means that the process of circulation switching should be a dynamic process, i.e., gyrotropic motion of the vortex core driven by time-dependent strain as described by Ostler *et al.*³⁰ and by electric pulses as described by Shiota *et al.*³¹ and the effect of dynamic strain reported in Foerster *et al.*³² We speculate that applying the electric field across the sample is equivalent to applying a pulsed strain on the magnetic disks. This may result in a similar circulation switching process that has been proposed in the literature recently for magnetic field pulses^{33,34} or for the core orientation switching by time-varying strain.³⁰ Because of the randomness involved during the ferroelectric domain switching process, the exact profile (strength, duration, and shape) of these strain pulses is unknown. Further theoretical and/or simulation work is needed from the community to confirm this observation. Nevertheless, the existence of the magnetic vortex circulation switching by the electric field is a promising direction towards the electric control of magnetization.

In summary, we have shown that strain induced EA switching in the Co ferromagnetic layer from the ferroelectric PMN-PT(011) substrate. The magnitude of the transferred strain can be tuned by inserting copper spacers of various thicknesses between the ferromagnetic layer and the ferroelectric substrate. When the ferromagnetic layer is patterned into nano-scale disks such that magnetic vortices are formed, non-volatile switching of the vortex circulation can be achieved by applying strain pulses of appropriate magnitude and/or length.

Financial support through National Key Research and Development Program of CHINA (No. 2016YFA0300804) National Science Foundation Grant No. DMR-1504568, Future Materials Discovery Program through the National Research Foundation of Korea (No. 2015M3D1A1070467), and Science Research Center Program through the National Research Foundation of Korea (No. 2015R1A5A1009962) is gratefully acknowledged. The operations of the Advanced

Light Source at Lawrence Berkeley National Laboratory are supported by the Director, Office of Science, Office of Basic Energy Sciences, and U.S. Department of Energy under Contract No. DE-AC02-05CH11231.

- ¹J. Åkerman, *Science* **308**, 508 (2005).
- ²F. Matsukura, Y. Tokura, and H. Ohno, *Nat. Nanotechnol.* **10**, 209 (2015).
- ³J. Ma, J. Hu, Z. Li, and C. W. Nan, *Adv. Mater.* **23**, 1062 (2011).
- ⁴B. Jang, J. Lee, K. Chu, P. Sharma, G. Kim, K. Ko, K. Kim, Y. Kim, K. Kang, H. Jang, H. Jang, M. Jung, K. Song, T. Koo, S. Choi, J. Seidel, Y. Jeong, H. Ohldag, J. Lee, and C. Yang, *Nat. Phys.* **13**, 189 (2017).
- ⁵J. Atulasimha and S. Bandyopadhyay, *Appl. Phys. Lett.* **97**, 173105 (2010).
- ⁶M. S. Fashami, J. Atulasimha, and S. Bandyopadhyay, *Nanotechnology* **23**, 105201 (2012).
- ⁷K. Roy, S. Bandyopadhyay, and J. Atulasimha, *Appl. Phys. Lett.* **99**, 063108 (2011).
- ⁸J. M. Hu and C. W. Nan, *Phys. Rev. B* **80**, 224416 (2009).
- ⁹N. A. Pertsev, *Phys. Rev. B* **78**, 212102 (2008).
- ¹⁰T. Nan, Z. Zhou, M. Liu, X. Yang, Y. Gao, B. A. Assaf, H. Lin, S. Velu, X. Wang, H. Luo, J. Chen, S. Akhtar, E. Hu, R. Rajiv, K. Krishnan, S. Sreedhar, D. Heiman, B. M. Howe, G. J. Brown, and N. X. Sun, *Sci. Rep.* **4**, 3688 (2014).
- ¹¹M. Liu, J. Hoffman, J. Wang, J. Zhang, B. Nelson-Cheeseman, and A. Bhattacharya, *Sci. Rep.* **3**, 1876 (2013).
- ¹²S. Zhang, Y. Zhao, X. Xiao, Y. Wu, S. Rizwan, L. Yang, P. Li, J. Wang, M. Zhu, H. Zhang, X. Jin, and X. Han, *Sci. Rep.* **4**, 3727 (2014).
- ¹³T. Wu, P. Zhao, M. Bao, A. Bur, J. L. Hockel, K. Wong, K. P. Mohanchandra, C. S. Lynch, and G. P. Carman, *J. Appl. Phys.* **109**, 124101 (2011).
- ¹⁴C. Thiele, K. Dörr, O. Bilani, J. Rödel, and L. Schultz, *Phys. Rev. B* **75**, 054408 (2007).
- ¹⁵T. Wu, A. Bur, K. Wong, P. Zhao, C. S. Lynch, P. K. Amiri, K. L. Wang, and G. P. Carman, *Appl. Phys. Lett.* **98**, 262504 (2011).
- ¹⁶M. Buzzi, R. V. Chopdekar, J. L. Hockel, A. Bur, T. Wu, N. Pilet, P. Warnicke, G. P. Carman, L. J. Heyderman, and F. Nolting, *Phys. Rev. Lett.* **111**, 027204 (2013).
- ¹⁷H. Ahmad, J. Atulasimha, and S. Bandyopadhyay, *Sci. Rep.* **5**, 18264 (2015).
- ¹⁸S. Finizio, M. Foerster, M. Buzzi, B. Krüger, M. Jourdan, C. A. F. Vaz, J. Hockel, T. Miyawaki, A. Tkach, S. Valencia, F. Kronast, G. P. Carman, F. Nolting, and M. Kläui, *Phys. Rev. Appl.* **1**, 021001 (2014).
- ¹⁹M. Schneider, H. Hoffmann, and J. Zweck, *Appl. Phys. Lett.* **79**, 3113 (2001).
- ²⁰Y. Gaididei, D. D. Sheka, and F. G. Mertens, *Appl. Phys. Lett.* **92**, 012503 (2008).
- ²¹S. Yakata, M. Miyata, S. Honda, H. Itoh, W. Wada, and T. Kimura, *Appl. Phys. Lett.* **99**, 242507 (2011).
- ²²V. Uhlíř, M. Urbánek, L. Hladík, J. Spousta, M.-Y. Im, P. Fischer, N. Eibagi, J. J. Kan, E. E. Fullerton, and T. Šikola, *Nat. Nanotechnol.* **8**, 341 (2013).
- ²³M. Tanase, A. K. Petford-Long, O. Heinonen, K. S. Buchanan, J. Sort, and J. Nogués, *Phys. Rev. B* **79**, 014436 (2009).
- ²⁴V. Sampath, N. D'Souza, D. Bhattacharya, G. M. Atkinson, S. Bandyopadhyay, and J. Atulasimha, *Nano Lett.* **16**, 5681 (2016).
- ²⁵J. Li, E. Jin, H. Son, A. Tan, W. N. Cao, C. Hwang, and Z. Q. Qiu, *Rev. Sci. Instrum.* **83**, 033906 (2012).
- ²⁶M. Weiler, A. Brandlmaier, S. Geprägs, M. Althammer, M. Opel, C. Bihler, H. Huebl, M. S. Brandt, R. Gross, and S. T. B. Goennenwein, *New J. Phys.* **11**, 013021 (2009).
- ²⁷J. Luo and S. Zhang, *Crystals* **4**(3), 306–330 (2014).
- ²⁸H. X. Fu and R. E. Cohen, *Nature* **403**, 281 (2000).
- ²⁹F. Fang, W. Yang, and X. Luo, *J. Am. Ceram. Soc.* **93**(11), 3916–3920 (2010).
- ³⁰T. A. Ostler, R. Cuadrado, R. W. Chantrell, A. W. Rushforth, and S. A. Cavill, *Phys. Rev. Lett.* **115**, 067202 (2015).
- ³¹Y. Shiota, T. Nozaki, F. Bonell, S. Murakami, T. Shinjo, and Y. Suzuki, *Nat. Mater.* **11**, 39 (2012).
- ³²M. Foerster, F. Macià, N. Statuto, S. Finizio, A. Hernández-Mínguez, S. Lendínez, P. V. Santos, J. Fontcuberta, J. M. Hernández, M. Kläui, and L. Aballe, preprint [arXiv:1611.02847v1](https://arxiv.org/abs/1611.02847v1).
- ³³M. Urbánek, V. Uhlíř, C.-H. Lambert, J. J. Kan, N. Eibagi, M. Vaňatka, L. Flajšman, R. Kalousek, M.-Y. Im, P. Fischer, T. Šikola, and E. E. Fullerton, *Phys. Rev. B* **91**, 094415 (2015).
- ³⁴R. Antos and Y. Otani, *Phys. Rev. B* **80**(R), 140404 (2009).